Glyconanogels as a versatile platform for the multivalent presentation of carbohydrates: from monosaccharides to dendritic glycostructures

Noelia de la Cruz,[§] Ana Sousa-Herves[§,‡,*] and Javier Rojo[§,*]

[§]Glycosystems Laboratory, Instituto de Investigaciones Químicas (IIQ), CSIC - Universidad de Sevilla, Av. Américo Vespucio 49, Seville 41092, Spain.
E-mail: ana.sousa@iiq.csic.es. E-mail: javier.rojo@iiq.csic.es

Abstract

Carbohydrate multivalent interactions play a key role in nature as efficient recognition tools for controlling a plethora of physiological and pathological events. These interactions are weak but the presence of multiple copies of ligands and receptors on biological surfaces leads to a multivalent recognition with enhanced selectivity and exponentially increased affinity. Here we report a simple and straightforward methodology for multivalent presentation of both simple monosaccharide ligands and complex dendritic glycostructures using polymeric nanogels (NGs). The interaction between the glycoNGs and a model lectin has been analysed by DLS and UV-Vis agglutination assays, showing that the introduction of glycodendrons with 3 and 9 mannose residues into the NGs results in a strong enhancement of the multivalency.

Keywords

Glyconanogel, Multivalency, Dendritic Glycostructures, Carbohydrates, Lectins

1. Introduction

Carbohydrate-protein interactions mediate many crucial biological events such as fertilization, cell growth and differentiation, inflammation, tumour progression, metastasis, and viral infection [1,2]. These interactions are typically characterised by a high selectivity, metal ion dependence and a low affinity, which is compensated in nature by the use of multivalency [1,3-5]. Thus, in contrast to weak monovalent binding, the clustered arrangement of carbohydrates on the cell or pathogen surface enables multiple interactions with lectins resulting in intensely enhanced binding affinities.

The synthesis of multivalent glycosylated architectures has been substantially developed in the past decades and has provided valuable advances toward deciphering the "sugar code" [6] in relation with the high complexity of oligosaccharides. In this regard, a variety of multivalent nanosized materials (dendrimers [7], polymers [8-10], nanoparticles [11-13], etc.) modified with several copies of carbohydrates have been designed as synthetic mimetics of natural glycoconjugates [14].

Our research group is particularly interested in the development of different multivalent scaffolds for the presentation of carbohydrates to receptors. In this context, in a joint effort with other research groups, we have reported the synthesis of several multivalent mannose-decorated glycoconjugates able to efficiently target and block the cellular receptor DC-SIGN (dendritic cell-specific intercellular adhesion molecule-3-grabbing non-integrin) [15]. Among all the conjugates prepared, the syntheses of giant glycofullerenes [16-18] and nanocarbon-based glycoconjugates [19] with antiviral activity have been recently reported. Despite those encouraging results, these artificial systems still face some limitations such as a relatively complex and expensive synthesis, which hampers their preparation in a multigram scale for clinical uses. In addition, the design of new scaffolds with different degrees of flexibility, sizes and geometries are crucial issues in the presentation of multivalent ligands [20-22]. In fact, they can even play a more significant role than multivalency itself in the carbohydrate-lectin recognition and binding events [23].

To improve the accessibility to carbohydrate multivalent systems and to overcome such drawbacks, the use of simpler and cheaper scaffolds, like polymeric micelles, nanoparticles or nanogels (NGs) can be considered. NGs are crosslinked, nanometric-scaled hydrogel particles with a tunable size and an interior network that is typically used for the incorporation of therapeutics. NGs are characterised by their soft and flexible nature, easy preparation, and high stability [24, 25].

Although polymeric NGs, including glycoNGs, have been mainly employed as drug and gene delivery vehicles [24, 26-30], some recent reports highlighted the potential of these nanostructures either to interact with cellular receptors [31] or to mimic them [32]. In these examples, the synthetic strategy involves the core-crosslinking of amphiphilic non-water soluble block copolymers containing protected carbohydrates or the conjugation of sugar units to multiple reactive sites at the surface of preformed NGs. One drawback of the latter methodology is that full substitution of nanostructures is normally impeded by steric hindrance and multistep protective group chemistry may be required.

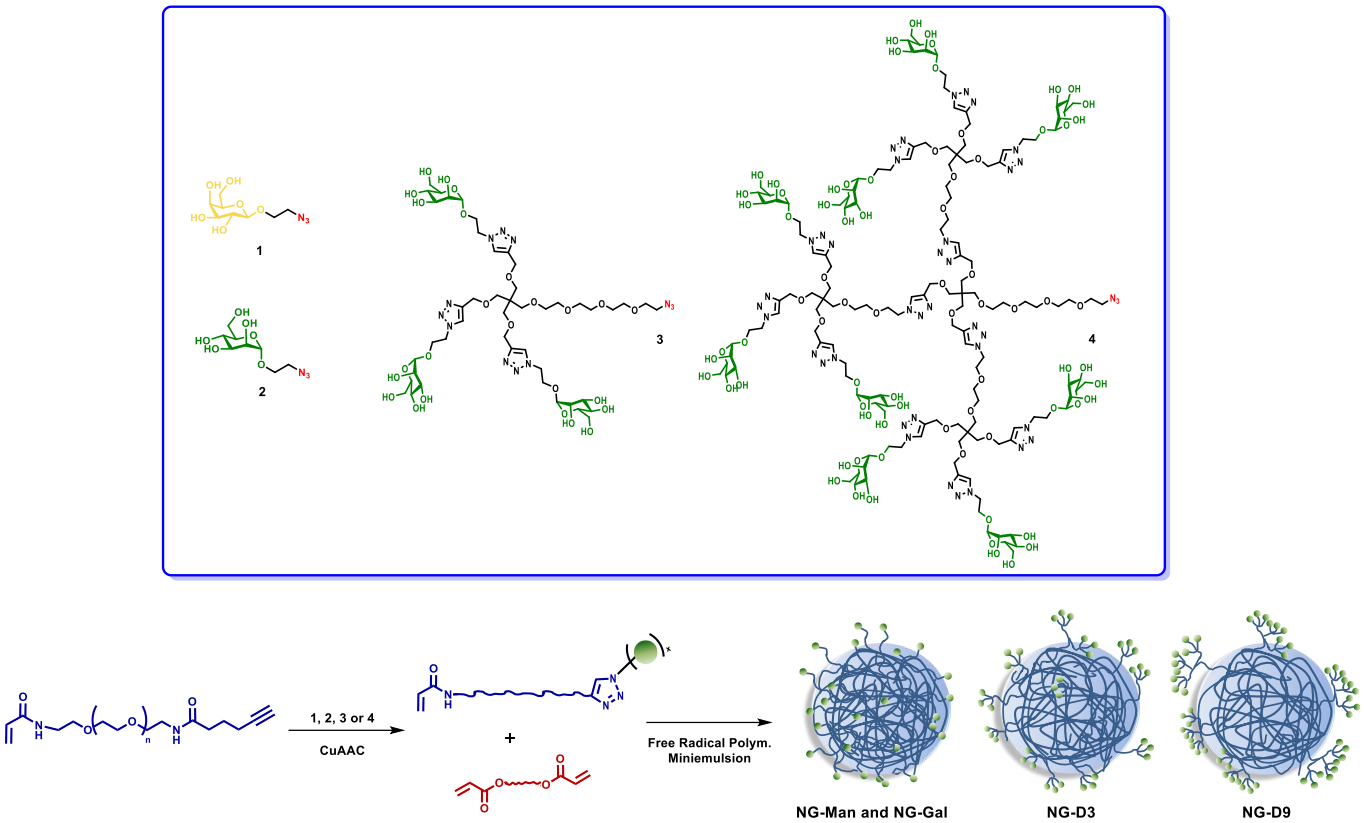

Fig. 1. Chemical structure of galactose (**1**) and mannosylated (**2-4**) ligands and an overview of the synthetic approach towards the preparation of multivalent glycoNGs.

Here we report a simple and straightforward approach to prepare glycoNGs with enhanced multivalency as versatile platforms for the presentation of carbohydrates. Using a common polymerisable intermediate, we can easily introduce different monovalent carbohydrates or readily enhance the multivalency of NGs by incorporating glycodendritic structures (Fig. 1). In this way, we can benefit from the multivalent and well-defined molecular architecture of dendrimers and the ease of synthesis of polymeric structures [33-35].

NGs have been prepared exclusively from linear, FDA-approved Poly(ethylene glycol) (PEG), a gold standard in the field of polymeric drug delivery [36]. The presence of PEG could result in an enhanced biocompatibility and longer circulation times in the blood stream (stealth properties) [36, 37]. To provide modularity, we propose a synthetic route involving a PEG-alkyne intermediate scaffold. In this way, the desired functional group or biomolecule can be easily incorporated into the polymerisable unit by means of the Cu(I)-catalysed azide-alkyne cycloaddition (CuAAC) [38, 39], (Fig. 1). Multivalency will be therefore achieved through the polymerization of a well-characterised carbohydrate-derivative monomer. This strategy offers superior structural control over the functionalization of preformed NGs because it allows the monitoring of complete carbohydrate coupling along with the affordable purification and characterisation of the resulting glycoconjugate. Importantly, with our modular synthetic strategy we can intensely enhance the NGs multivalency by simply introducing glycodendrons with 3 or 9 mannoses [40] (**3** and **4**, Fig. 1) into the polymerisable unit.

2. Results and discussion

2.1 Synthetic procedures.

Synthesis of the PEGylated building blocks. The synthesis of the PEG-carbohydrate **10a-d** polymerisable units is depicted in Fig. 2. In brief, the free NH_2 group of one of the distal ends of the PEG chain **6** was coupled with hexynoic acid using typical peptide chemistry to produce **7** on a large scale (quant. yield). Next, acrylate compound **9** was obtained by deprotection of the terminal Boc group with TFA (compound **8**, quant. yield), followed by reaction with acryloyl chloride in DMF (quant. yield). The resulting polymeric chain modified at one end with an acrylate group and at the other with an alkyne functionality was then submitted to CuAAC coupling (using $CuSO_4$ and sodium ascorbate) with the unprotected carbohydrates (**2)** and glycodendrons (**3, 4)** to yield mannosylated compounds **10b-d** with different valencies in good yields (62-82%). The azidogalactose **1** was also introduced with the aim of preparing control NGs for further interaction studies with lectins. Importantly, alongside NMR spectroscopy (see Electronic Supplementary Information, ESI), the correct structure of compounds **9** to **10d** could be further confirmed by MALDI-TOF spectrometry, which showed a series of 44 Da spaced peaks distinctive of PEG along with the expected increase in mass (ESI).

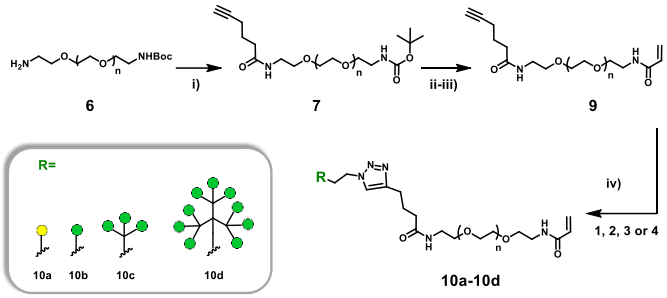

Fig. 2. Synthesis of the polymerisable building blocks. Reagents and conditions: (i) hexynoic acid, HATU, DIPEA, rt, overnight (quant.); (ii) TFA/CH_2Cl_2, rt, 2 h, (**8**, quant.); (iii) acryloyl chloride, Et_3N, DMF, (quant.); (iv) $CuSO_4 \cdot 5H_2O$, sodium ascorbate, *t*-BuOH/H_2O, rt, 48 h (**10a** 80%; **10b** 82%, **10c** 67%, **10d** 62%).

2.2 Preparation of the GlycoNGs. Once the PEG-carbohydrate **10a-d** polymerisable units were synthesised, NGs displaying multiple copies of carbohydrates could be prepared. With this aim, we have employed free radical polymerisation, using inverse miniemulsion to template the NGs formation. Miniemulsion technique allows the creation of stable nanodroplets (typically with sizes between 50-500 nm) in a continuous phase by applying high shear stress like ultrasonication [41]. Subsequently, polymerisation takes place inside the nanodroplets. Monomers (**10a-d**, 1 eq), PEG-diacrylate crosslinker (0.15 eq) and ammonium persulfate (APS; 1.15 eq) were dissolved in MilliQ water. The ratio monomers/crosslinker/initiators was determined experimentally. The aqueous solution was then mixed with cyclohexane containing non-ionic surfactants [42]. After application of ultrasonication, the resulting solution was flushed with Ar and tetramethylethylenediamine (TEMED) was added to initiate the polymerisation. After purification in cyclohexane and MilliQ water, NGs of galactose (NG-Gal), NGs of mannose (NG-Man), NGs of 3 mannoses dendron (NG-D3) and NGs of 9 mannoses dendron (NG-D9) were obtained (Fig. 1).

2.3 Characterisation of the GlycoNGs.

Firstly, NGs solutions were measured by dynamic light scattering (DLS), which revealed the presence of particles with similar hydrodynamic diameters (150-180 nm) and narrow size distributions in all cases, suggesting that the NG sizes are mainly defined by the miniemulsion droplet size. In such a case, it would not be expected that the type of carbohydrates could have an impact on the hydrodynamic ratio of the nanogels (Fig. 3 and Table 1).

Table 1. NGs sizes and polydispersity index (PDI) by DLS

Nanogel	Polymeric precursor	Hydrodynamic diameter (nm)	PDI
NG-Gal	10a	172.2 ± 1.5	0.19
NG-Man	10b	178.4 ± 7.4	0.20
NG-D3	10c	151.0 ± 2.6	0.29
NG-D9	10d	177.0 ± 1.0	0.33

Scanning electron microscopy (SEM) and transmission electron microscopy (TEM) images of NG-Man and NG-D9 were also acquired (Fig. 3). TEM and SEM showed particles with a predominant spherical morphology and mean diameters in good agreement with DLS. More specifically, in the case of NG-Man no significant difference was observed between DLS and TEM data (178 ± 7.4 *vs*. 166 ± 45 nm, respectively). For NG-D9, TEM showed a higher diameter than DLS, but also a larger SD (275.6 ± 111 *vs*. 177.0 ± 1.0). Interestingly, glycoNGs revealed completely stable in solution at 4 ºC for at least 1 year, and could be freeze dried for their storage, which expands their applicability as potential therapeutics.

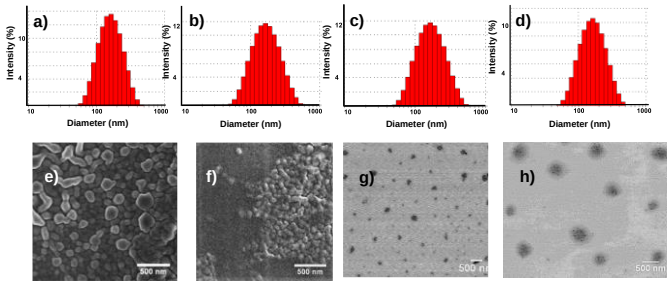

Fig. 3. DLS size histogram of NG-Gal (a), NG-Man (b), NG-D3 (c), and NG-D9 (d) in H_2O. SEM images of NG-Man (e) and NG-D9 (f). TEM images of NG-Man (g) and NG-D9 (h).

The amount of mannoses in the glycoNGs could be estimated by the sulfuric acid–UV method [43] after performing a calibration curve (Fig. S1, ESI). According to this method, NGs prepared from simple monosaccharides NG-Man and NG-Gal contain 3.7% and 4.0% (wt./wt.) of galactose and mannose, respectively. These amounts are approximately 60% of the maximum theoretical amounts of monosaccharides in monomers **10a** and **10b** (6.4%). Interestingly, we observed a similar result for the NGs prepared from the much bulkier dendritic blocks NG-D3 and NG-D9. The amount of tri/nonamannosylated glycodendrons in NGs are 11.4% and 22.1%, respectively, corresponding to approximately 45% of the theoretical amount in monomers **10c** and **10d** (27.7% and 54.8%). These results demonstrate that approximately 50% of the acrylate glycopolymers **10a-d** are introduced in the NGs after polymerisation in all cases, suggesting a good control over the NG synthesis and reproducibility. These values are summarised in Table 2.

Table 2. Theoretical (th.) and experimental (exp.) amounts of carbohydrates (wt.%) in polymeric precursors and the corresponding GlycoNGs.

Nanogel	% Glycosylated ligand (polymer, th.)	% Glycosylated ligand (NGs, exp.)	% Carbohyd. (NGs, th.)	% Carbohyd. (NGs, exp.)
NG-Gal	6.4	4.0	6.4	4.0
NG-Man	6.4	3.7	6.4	3.7
NG-D3	27.7	11.4	12.5	5.1
NG-D9	54.8	22.1	23.5	9.5

2.4 Evaluation of the interaction of the GlycoNGs with the model lectin Concanavalin A.

While nanoscale scaffolds provide advantages such as the multivalent presentation of ligands, the localized clusters of ligands in the NGs prepared from the linear-dendritic blocks could also enhance binding due to localized high concentrations or a "proximity effect" [34,44]. With the aim of analysing the actual capacity of the NGs to interact with lectins, and to elucidate if there is any multivalent-dependent activity, preliminary binding studies with the model lectin Concanavalin A (ConA) were performed by DLS and UV-spectroscopy. ConA is a homotetramer at physiological pH that recognises mannoses but not galactoses, so galactosylated nanogels (NG-Gal) were used as a negative control. We first measured the size of the well-defined ConA homotetramer in buffer at pH 7.2 by DLS (6.7 ± 0.4 nm, PDI 0.19, Fig. 4a) and subsequently monitored its agglutination by the addition of increasing amounts of the different glycoNGs (Fig. 4).

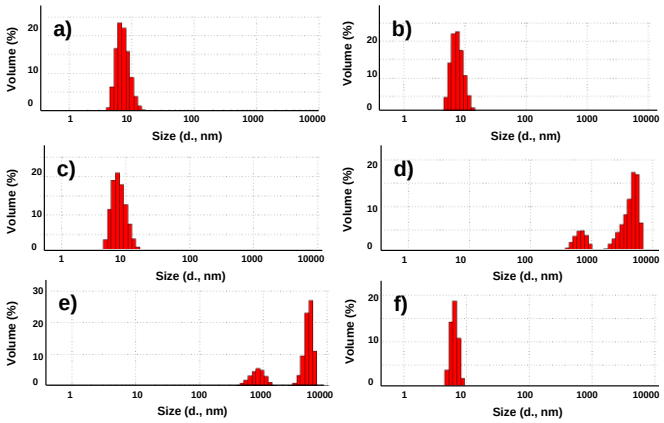

Fig. 4. DLS volume size histograms (0.1 M Tris-HCl pH 7.2 , 0.9 M KCl, 1 mM $MnCl_2$, and 1 mM $CaCl_2$) of: a) ConA (0.5 mg/mL), b) ConA + 10 μg of NG-Gal, c) ConA + 10 μg of NG-Man. d) ConA + 10 μg of NG-D3, e) ConA + 10 μg of NG-D9, and f) ConA + 10 μg of NG-D9 + α-D-mannose.

As shown in Fig. 4 and Fig. 5a, DLS allowed the detection of particles with higher size immediately upon the addition of very small amounts of NGs. The results revealed an increased binding capacity for the NGs with enhanced multivalency NG-D3 and NG-D9 (Fig. 4d and 4e, Fig. 5a). Thus, these NGs rapidly aggregate with ConA forming large species from a NG concentration of *ca.* 1 μg. On the contrary, in the case of the lower valency NG, NG-Man, a 900-fold higher concentration of NGs was necessary to observe a significant effect (Fig. S2, ESI). No aggregation was observed for the control NG-Gal at any concentration (Fig. 4, 5 and S2), proving the specific lectin-binding properties of the NGs. In accordance with the reversible nature of the interaction, the addition of a saturated solution of α-D-mannose completely broke the aggregates (Fig. 4f).

Interestingly, DLS binding experiments performed on a per sugar basis (i.e. considering the carbohydrate wt.% of the different systems) showed that NG-D9 could rapidly form aggregates while no binding was observed for the NG-Man even at much higher sugar concentrations (40 *vs*. 200 ng, respectively, Fig. 5b). Furthermore, although NG-D9 seemed to interact with ConA at slightly lower concentrations than NG-D3, this effect was not particularly prominent. In this case, the increase of the valency does not have a strong rise in the activity, as previously observed for other multivalent compounds [45].

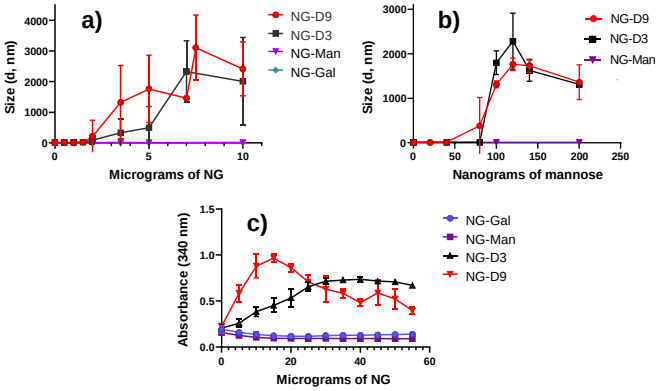

Fig. 5. Agglutination assays by DLS (25 ºC) as a function of NG amount (a) and per-sugar basis (b). UV agglutination assays (c).

A similar result was observed when UV-Vis turbidimetry assays were performed for higher NGs concentrations (up to 60 μg, Fig. 5c). In this case, an increase in the absorbance or even precipitation was observed when aggregates between the lectin and the glycoNGs were formed. The addition of NG-D9 to a ConA solution showed the formation of large aggregates at lower NG concentrations than for the NG-D3. Again, no changes in the absorbance could be observed for NG-Man and NG-Gal in this concentration range. In fact, NG-Man did not show any sign of aggregation even after the addition of 1.25 mg of the NG. Higher concentration ranges could not be analysed by this method due to precipitation of the ConA-NGs aggregates. The reversibility of the interaction was again verified by the addition of a saturated solution of α-D-mannose, which completely removed turbidity.

3. Experimental

3.1 Materials and Methods.

Solvents were HPLC grade and used as received unless otherwise stated. Size exclusion chromatography was done with Sephadex LH20 (GE Healthcare). Thin-layer chromatography (TLC) was done on silica plates (Merck). BocNH-PEG-NH_2 (MW 3000, PDI 1.03. M_p 3271 by MALDI-TOF, HABA) was obtained from Iris Biotech. PEG di-acrylate (M_n 575), 1-[bis(dimethylamino)methylene]-1H-1,2,3-triazolo[4,5-b]pyridinium 3-oxid hexafluorophosphate (HATU), acryloyl chloride, dry N, N-diisopropylethylamine (DIPEA), trifluoroacetic acid (TFA), QuadraSil® MP, Tween® 80, Span® 80, ammonium persulfate (APS), tetramethylethylenediamine (TEMED) and ConA were purchased from Sigma Aldrich. 2-Azidoethyl α-D-mannopyranoside [46], 2-azidoethyl β-D-galactopyranoside and glycodendrons of 3 and 9 units of α-D-mannopyranoside were synthesized as previously described [36]. Amicon Ultra-15 centrifugal filters (MWCO 30 and 50 KDa) were obtained from Millipore. Ultrafiltration was performed on stirred cells with Amicon® YM5 membranes (MWCO 5 KDa, Millipore). NMR experiments were performed in a Bruker Advance DRX 400 instrument. NMR chemical shifts are reported in ppm (δ units) downfield from the $CDCl_3$ signal

or the HOD peak (D_2O). 2D experiments (COSY and HSQC) were performed when necessary. NMR spectra were analysed with MestreNova software.

3.2 MALDI-TOF MS measurements.

MALDI-TOF MS experiments were carried out in a bench-top Microflex LRF (Bruker Daltonics, Inc.) MALDI-TOF MS operating in linear mode. Different matrixes were employed, depending on the sample. For the starting polymer **6**, the matrix employed was 2-(4-hydroxyphenylazo)benzoic acid (HABA) and NaCl was used as cationisation agent. In the case of compounds **9** and **10a** the matrix used was trans-2-[3-(4-tert-Butylphenyl)-2-methyl-2-propenylidene]malononitrile (DCTB). For the rest of compounds, the matrix employed was α-Cyano-4-hydroxycinnamic acid (HCCA) and trifluoroacetic acid (TFA) was used as cationisation agent. The heavier compound, **10d**, flew with more difficulty, and higher laser power had to be applied. As a result, fragmentation (attributed to PEG) during the MALDI experiment was observed.

3.3 Synthesis of the polymerisable building blocks.

*Alkyne-PEG-NHBoc (**7**)*. NH_2-PEG-NHBoc (**6**) (100 mg, 0.032 mmol) was dissolved in dry DMF (2 mL) under Ar. Dry N, N-diisopropylethylamine (DIPEA, 17 µL, 0.098 mmol) was added to the solution. Separately, 5-hexynoic acid (11 µL, 0.098 mmol) and HATU (37 mg, 0.098 mmol) were dissolved in dry DMF (2 mL) and stirred for 10 min. Subsequently, this solution was added to the NH_2-PEG-NHBoc solution and the reaction mixture was stirred overnight (on) at room temperature (rt). After that time, the solvent was evaporated under vacuum and purification was performed in a Sephadex LH20 column in MeOH. The pure compound **7** was obtained as a white solid (101 mg, quantitative). ^{1}H NMR (400 MHz, $CDCl_3$) δ: 6.25 (br s, 1H), 5.03 (br s, 1H), 3.82-3.34 (m, ~ 315H), 3.29-3.17 (m, 2H), 2.26 (t, *J* = 7.4 Hz, 2H), 2.19 (td, *J* = 7.4 Hz, *J* = 2.6 Hz, 2H), 1.94 (t, *J* = 2.6 Hz, 1H), 1.83-1.76 (m, 2H), 1.38 (s, 9H). ^{13}C NMR (100 MHz, $CDCl_3$) δ: 172.2, 156.0, 83.6, 79.1, 78.4, 73.1, 70.5, 70.2, 69.8, 69.2, 67.9, 62.8, 40.3, 39.1, 34.9, 28.4, 24.2, 17.9.

*Alkyne-PEG-$NH_3^+CF_3COO^-$ (**8**)*. Alkyne-PEG-NHBoc (101 mg, 0.032 mmol) was dissolved in CH_2Cl_2 (2.5 mL) and TFA (0.5 mL). After 2 h stirring at rt, the solvent was evaporated under vacuum and the crude product was purified by Sephadex LH20 column in MeOH. The unprotected alkyne-PEG-amino intermediate **8** was obtained as a white solid (98 mg, quantitative). ^{1}H RMN (400 MHz, $CDCl_3$) δ: 7.83 (br s, 3H), 6.32 (br s, 1H), 4.02-3.28 (m, ~ 300H), 3.14 (t, *J* = 5.0 Hz, 2H), 2.27 (t, *J* = 7.4 Hz, 2H), 2.21 (td, *J* = 6.9 Hz, *J* =2.6 Hz, 2 H), 1.95 (t, *J* = 2.6 Hz, 1H), 1.87-1.75 (m, 2H). ^{13}C NMR (100 MHz, $CDCl_3$) δ: 172.3, 83.6, 70.5, 70.3-69.9, 69.9, 69.1, 67.1, 40.1, 39.1, 34.9, 24.2, 17.9.

*Alkyne-PEG-acrylate (**9**)*. Alkyne-PEG-$NH_3^+CF_3COO^-$ (98 mg, 0.032 mmol) was dissolved in dry DMF (5 mL) under Ar and triethylamine (24 µL, 0.175 mmol) was added. The solution was cooled down to 0ºC and after 10 min acryloyl chloride (13 µL, 0.160 mmol) was slowly added. The mixing was stirred on at rt, protected from light. After that time, DMF was removed under vacuum and the reaction mixture was purified by Sephadex LH20 in MeOH (*p*-anisaldehyde as stain). The polymerisable building block **9** was obtained as a white solid (100 mg, quantitative). After NMR characterisation, the product was immediately dissolved in MeOH and stored at rt protected from light. ^{1}H NMR (400 MHz, $CDCl_3$) δ: 6.71 (br s, 1H), 6.37 (br s, 1H), 6.30-6.07 (m, 2H), 5.58 (dd, *J* = 10.1 Hz, 1.8 Hz, 1H), 3.86-3.30 (m, ~ 315H), 2.29 (t, *J* = 7.4 Hz, 2H), 2.22 (td, *J* = 7.4 Hz, *J* = 2.6 Hz, 2H), 1.96 (t, *J* = 2.6 Hz, 1H), 1.88-1.77 (m, 2H). ^{13}C NMR (100 MHz, $CDCl_3$) δ: 172.3, 165.6, 131.1, 125.9, 83.6, 70.5, 70.2, 70.1, 69.9, 69.8, 69.1, 39.3, 39.2, 34.9, 24.2, 17.9. MALDI-TOF MS (DCTB): m/z Calcd: M_p 3319; Found: M_p 3313.

3.4 General procedure for the CuAAC coupling.

Alkyne-PEG-acrylate **9** (1 eq) and carbohydrates **1-2** or glycodendrons **3-4** (2.5 eq) were dissolved in *t*-BuOH/H_2O (1:1, 0.05 M final concentration of polymer). Fresh solutions of $CuSO_4$ pentahydrate and sodium ascorbate were added and the mixture was stirred at rt for 48 h protected from light. Afterwards, a small amount of Quadrasil® MP was added to the crude product and the mixture was shaken for 20 min to remove the copper catalyst. After filtration, the crude product was purified by Sephadex LH20 in MeOH to yield compounds **10a-c** or by ultrafiltration in H_2O with YM5 membranes for **10d**.

*Galactose-PEG-acrylate (**10a**)*. Alkyne-PEG-acrylate **9** (53 mg, 0.017 mmol) and 2-azidoethyl β-D-galactopyranoside (11 mg, 0.043 mmol) were dissolved in *t*BuOH/H_2O. Fresh solutions of $CuSO_4$ pentahydrate (0.011 mmol) and sodium ascorbate (0.056 mmol) were added and after 48 h of reaction time following the general procedure described above, **10a** was obtained (46 mg, 80% yield). ^{1}H NMR (400 MHz, D_2O) δ: 7.91 (s, 1H), 6.36-6.15 (m, 2H), 5.79 (dd, *J* = 9.9 Hz, *J* = 1.8 Hz, 1H), 4.66 (t, *J* = 5.1 Hz, 2H), 4.36 (d, *J* = 7.7 Hz, 1H), 4.34-4.25 (m, 1H), 4.17-4.06 (m, 1H), 3.96-3.45 (m, ~ 436H), 3.42-3.31 (m, 2H), 2.75 (t, *J* = 7.4 Hz, 2H), 2.31 (t, *J* = 7.4 Hz, 2H), 2.04-1.91 (m, 2H). ^{13}C NMR (100 MHz, D_2O) δ: 176.3, 168.4, 147.3, 129.9, 127.4, 123.6, 103.0, 75.1, 72.6, 70.8, 70.7, 70.5, 69.6, 68.8, 68.7, 68.5, 68.1, 67.0, 60.9, 50.2, 39.0, 38.9, 35.0, 25.0, 24.0. MALDI-TOF MS: MS (DCTB): m/z Calcd: M_p 3568, Found: M_p 3481

*Mannose-PEG-acrylate (**10b**)*. Alkyne-PEG-NH-acrylate **9** (122 mg, 0.039 mmol) and 2-azidoethyl α-D-mannopyranoside (24 mg, 0.098 mmol) were dissolved in *t*BuOH/H_2O. Fresh solutions of $CuSO_4$ pentahydrate (0.026 mmol) and sodium ascorbate (0.129 mmol) were added and after 48 h of reaction time following the general procedure described above, **10b** was obtained (108 mg, 82% yield). ^{1}H NMR (400 MHz, D_2O) δ: 7.89 (s, 1H), 6.36-6.16 (m, 2H), 5.79 (dd, *J* = 10.0 Hz, *J* = 1.6 Hz, 1H), 4.79 (under D2O, 1H), 4.69-4.61 (m, 2H), 4.17-4.05 (m, 1H), 4.02-3.46 (m, ~ 380H), 3.39 (t, *J* = 5.3 Hz, 2H), 3.06-2.96 (m, 1H), 2.75 (t, *J* = 7.5 Hz, 2H), 2.31 (t, *J* = 7.4 Hz, 2H), 2.04-1.90 (m, 2H). ^{13}C NMR (100 MHz, D_2O) δ: 176.2, 168.6, 129.9, 127.4, 123.6, 99.5, 85.2, 72.8, 71.6, 70.4, 69.6, 68.8, 68.7, 67.5, 66.3, 65.5, 60.6, 60.4, 49.9, 39.0, 38.9, 35.0, 25.1, 23.9. MALDI-TOF MS: MS (HCCA): m/z Calcd: M_p 3568, Found: M_p 3740

*Glycodendron of 3 mannoses-PEG-acrylate (**10c**)*. Alkyne-PEG-NH-acrylate **9** (97 mg, 0.031 mmol) and glycodendron of 3 mannoses (**3**, 93 mg, 0.078 mmol) were dissolved in *t*-BuOH/H_2O. Fresh solutions of $CuSO_4$ pentahydrate (0.021 mmol) and sodium ascorbate (0.102 mmol) were added and after 48 h of reaction time following the general procedure described above, **10c** was obtained (90 mg, 67% yield). ^{1}H NMR (400 MHz, D_2O) δ: 8.05 (s, 3H), 7.85 (s, 1H), 6.36-6.16 (m, 2H), 5.79 (dd, *J* = 10.0 Hz, *J* = 1.6 Hz, 1H), 4.79 (under D_2O, 3H), 4.71-4.63 (m, 4H), 4.62-4.54 (m, 7H), 4.16-3.33 (m, 374H), 3.15-3.03 (m, 3H), 2.72 (t, *J* = 7.6 Hz, 2H), 2.30 (t, *J* = 7.4 Hz, 2H), 2.03-1.88 (m, 2H). ^{13}C NMR (100 MHz, D_2O) δ: 176.1, 168.5, 147.4, 144.3, 129.9, 127.4, 125.4, 123.7, 99.6, 86.2, 72.8, 71.7, 70.5, 69.9, 69.6, 68.8, 68.7,

68.3, 67.5, 66.4, 65.5, 63.6, 60.7, 50.0, 49.9, 44.8, 39.0, 38.9, 35.0, 25.1, 24.0. MALDI-TOF MS: MS (HCCA): m/z Calcd: M_p 4517, Found: M_p 4505.

*Glycodendron of 9 mannoses-PEG-acrylate (**10d**)*. Alkyne-PEG-NH-acrylate **9** (66 mg, 0.021 mmol) and glycodendron of 9 mannoses (**4**, 200 mg, 0.053 mmol) were dissolved in *t*-BuOH/H_2O. Fresh solutions of $CuSO_4$ pentahydrate (0.014 mmol) and sodium ascorbate (0.069 mmol) were added and after 48 h of reaction time following the general procedure described above, **10d** was obtained (90 mg, 62% yield). ^{1}H NMR (400 MHz, D_2O) δ: 8.02 (s, 9H), 7.97 (s, 3H), 7.83 (s, 1H), 6.36-6.15 (m, 2H), 5.78 (dd, *J* = 9.9 Hz, *J* = 1.6 Hz, 1H), 4.79 (under D_2O, 9H), 4.67-4.60 (m, 12H), 4.58-4.50 (m, 20H), 4.50-4.46 (m, 3H), 4.15-4.01 (m, 9H), 3.96-3.27 (m, 450H), 3.15-3.03 (m, 9H), 2.70 (t, *J* = 7.4 Hz, 2H), 2.28 (t, *J* = 7.4 Hz, 2H), 1.99-1.86 (m, 2H). ^{13}C NMR (100 MHz, D_2O) δ: 176.2, 168.4, 144.3, 144.2, 129.9, 127.4, 125.3, 125.1, 123.6, 99.6, 72.8, 70.5, 69.9, 69.6, 68.9, 68.8-68.7, 68.2, 67.5, 66.4, 65.4, 63.6, 60.7, 50.0, 49.8, 44.8, 39.0, 38.9, 35.0, 25.1, 24.0. MALDI-TOF MS: MS (HCCA): m/z Calcd: M_p 7101, Found: M_p 7137.

3.5 General procedure for the preparation of NGs.

NGs were synthesized at rt by free radical polymerization using a miniemulsion technique to template NGs formation. In a representative example, Mannose-PEG-acrylate (10b, 23 mg, 6.8 µmol, 1 eq), PEG-diacrylate (0.5 µL, 0.97 µmol, 0.15 eq) and APS (1.79 mg, 7.8 µmol, 1.15 eq) were dissolved in 250 mL of MilliQ water and mixed with 15 mL of cyclohexane containing Tween® 80 (100 mg) and Span® 80 (300 mg). The mixture was then ultrasonicated with a Branson Digital Sonifier (5 × 30 seconds) yielding a stable emulsion. DLS measurements were performed right after ultrasonication to check the size and dispersity of the nanodroplets. Next, the solution was flushed with Ar and TEMED (1.15 µL, 7.8 µmol, 1.15 eq) was added. The resulting solution was stirred on under Ar atmosphere. Afterwards, 30 mL of cyclohexane were added, and the solution was centrifuged (1 h, 6000 rpm). A gel-like precipitate could be observed. The supernatant was removed and 15 mL more of cyclohexane were added. The solution was centrifuged again (30 min, 6000 rpm, the procedure was done twice). After complete solvent drying, MilliQ water was added and the resulting solution was washed using Amicon Ultra-15 centrifugal filters (MWCO 30 KDa). The resulting NGs (3.8 mg) were either freeze-dried or kept in solution at 4 ºC for their storage. The rest of the GlycoNGs were prepared following this methodology.

3.6 DLS.

DLS measurements were performed on a Malvern Nano ZS (Malvern Instruments, U.K.) operating at 633 nm with a 173º scattering angle. NGs were dissolved at 2 mg/mL in MilliQ water and the solutions were filtered through a 0.45 µm nylon filter before the measurements. The mean values stated in Table 1 resulted from at least 3 measurements.

3.7 SEM and TEM.

SEM and TEM analyses were performed on a Hitachi S4800 SEM-FEG microscope of high resolution. The microscope was equipped with a Bruker-X Flash-4010 EDX detector with a resolution of 133 eV (at the MnKα line), and a detector with sample holder to work in transmission mode (STEM-in-SEM). A Leica EM ACE600 sputter coater (Cr) was employed. For TEM and SEM studies a drop of the NGs solution in MilliQ water (0.02-0.04 mg/mL) was settled on a Formvar precoated copper grid (400 mesh; Aname S. L.) and allowed to dry at rt for 12 h. For TEM measurements, statistical analysis was performed using Image J software. NG-Man (7.2 × 6.7 µm image). Total Count: 25. Diameter: 166.04 ± 45 nm. NG-D9 (5.9 × 4.4 µm image). Total Count: 13. Diameter: 275.6 ± 111 nm.

3.8 Determination of the amount of carbohydrates in the NGs.

The amount of carbohydrates in the NGs was estimated following a procedure described elsewhere [43]. In brief, the amount of carbohydrate could be determined by UV-Vis spectroscopy in H_2SO_4/H_2O (λ = 315 nm) after performing a calibration curve for each glycosystem, namely galactose, mannose, dendron of 3 mannoses, and dendron of 9 mannoses (Fig. S1). The weight percentage of each glycosystem could be estimated by the following equation, where $W_{glycosystem}$ and W_{NG} stand for the glycosystem weight and the weight of the NGs, respectively:

$$\text{Glycosystem loading (wt.\%)} = (W_{glycosystem} / W_{NG}) \times 100$$

The amount of glycodendrons in each NG can be transformed into amount of mannoses, considering the MW of the polymeric precursor and the weight of mannoses on it.

3.9 Lectin binding assays by DLS.

ConA agglutination assays were used to investigate the ability of the glycoNGs to bind mannose-binding lectins by DLS. ConA was dissolved at 0.5 mg/mL in 0.1 M Tris-HCl pH 7.2 containing 0.9 M KCl, 1 mM $MnCl_2$ and 1 mM $CaCl_2$. 500 µL of ConA were placed into a DLS microcuvette, and DLS measurements for the lectin alone were performed. Afterwards, increasing amounts (starting from 5 µL) of a solution of NG at 0.1 mg/mL were added and DLS measurements were recorded 5 min after mixing. For DLS experiments carried out on a per-sugar basis, NGs solutions of 4 µg/mL of mannose (or galactose for control NGs) were prepared. The values represented in Fig. 5 correspond to the mean of 3 measurements in 3 independent experiments with error bars corresponding to the standard errors of the mean. The data was analysed using GraphPad Prism v8.2.1.

3.10 Lectin binding by turbidimetry assays.

A solution of each glycoNG (142.8 µg/mL in 0.1 M Tris-HCl, 0.9 M KCl, 1 mM $MnCl_2$, 1 mM $CaCl_2$, pH=7.2) was sequentially added, in 35 µL portions, to a solution of ConA (350 µL, 0.45 mg/ml in the same buffer). After each addition, the resulting mixture was allowed to stand for 5 min before the absorbance was measured at 340 nm and the following NG addition was performed. The values represented in Fig. 5c correspond to 3 independent experiments with error bars corresponding to the standard errors of the mean. To determine the most suitable wavelength to measure the ConA-NGs aggregates (340 nm), a complete absorption spectrum was first acquired.

4. Conclusions

In conclusion, we have described the preparation of PEG-based, flexible glycoNGs modified with several mannose copies. The proposed methodology is easy and modular, allowing on-demand sugar decoration and the enhancement of the NGs multivalency by introducing glycodendrons with 3 and 9 copies of mannose. In addition, other scaffolds with different degrees

of flexibility, sizes or geometries could be introduced into the NGs using this simple approach. Agglutination assays with the model lectin ConA have been performed by DLS and UV spectroscopy, showing that the NGs prepared from the glycodendritic precursors displayed an enhanced capacity to interact with the lectin in solution while control NGs showed no activity at all. The simplicity of the described synthesis, together with the favourable properties of PEGylated nanostructures and the capability of the NGs to selectively interact with biological receptors, make these glycoNGs promising scaffolds in nanobiotechnology.

Conflicts of interest

There are no conflicts to declare.

Acknowledgements

This work was financially supported by MINECO (CTQ2017-86265-P, and IJCI-2015-23272), the Andalucia Talent Hub program (291780) and ISCIII RETICS ARADyAL (RD16/0006/0011). Grants were co-funded by the European Regional Development Fund (ERDF). A.S.-H. and N.d.l.C thank MINECO for their Juan de la Cierva-Incorporacion and FPI contracts, respectively.

Author Contributions

The manuscript was written through contributions of all authors. All authors have given approval to the final version of the manuscript.

Present Address

‡ Departamento de Química Inorgánica, Orgánica y Bioquímica, Facultad de Farmacia, Universidad de Castilla-La Mancha, C/José María Sánchez Ibañez s/n, 02071, Albacete, Spain

References

[1] Y.C. Lee, R.T. Lee, Carbohydrate-Protein Interactions: Basis of Glycobiology, Acc. Chem. Res. 28 (1995) 321-327. https://doi.org/10.1021/ar00056a001

[2] A. Varki, Biological roles of glycans, Glycobiology, 27, 2017, Pages 3–49, https://doi.org/10.1093/glycob/cww086

[3] C. Fasting, C.A. Schalley, M. Weber, O. Seitz, S. Hecht, B. Koksch, J. Dernedde, C. Graf, E.-W. Knapp, R. Haag, Multivalency as a Chemical Organization and Action Principle, Angew. Chem. Int. Ed. 51 (2012) 10472-10498. https://doi.org/10.1002/anie.201201114

[4] L. L. Kiessling, T. Young, T. D. Gruber and K. H. Mortell, in *Glycoscience*, eds. B. Fraser-Reid, K. Tatsuta and J. Thiem, Springer Berlin Heidelberg, 2008, pp 2483-2523.

[5] J. J. Lundquist, and E. J. Toone, The Cluster Glycoside Effect, Chem. Rev. 102 (2002) 555-578. https://doi.org/10.1021/cr000418f

[6] H. J. Gabius, *The sugar code : fundamentals of glycosciences*, Wiley-VCH ; John Wiley Weinheim; Chichester, 2009.

[7] Y.M. Chabre, R. Roy, Recent Trends in Glycodendrimer Syntheses and Applications, Curr. Top. Med. Chem 8 (2008) 1237-1285.

[8] S.R.S. Ting, G. Chen, M.H. Stenzel, Synthesis of glycopolymers and their multivalent recognitions with lectins, Polym. Chem. 1 (2010) 1392-1412. https://doi.org/10.1039/C0PY00141D

[9] Y. Miura, Y. Hoshino, H. Seto, Glycopolymer Nanobiotechnology, Chem. Rev. 116. (2016) 1673-1692. https://doi.org/10.1021/acs.chemrev.5b00247

[10] C. R. Becer, L. Hartmann, Glycopolymer Code: Synthesis of Glycopolymers and their Applications, The Royal Society of Chemistry, 2015.

[11] A.P.P. Kröger, M.I. Komil, N.M. Hamelmann, A. Juan, M.H. Stenzel, J.M.J. Paulusse, Glucose Single-Chain Polymer Nanoparticles for Cellular Targeting, ACS Macro Lett. 8 (2019) 95-101. https://doi.org/10.1021/acsmacrolett.8b00812

[12] G. Yilmaz, C.R. Becer, Glyconanoparticles and their interactions with lectins, Polym. Chem. 6 (2015) 5503-5514. https://doi.org/10.1039/C5PY00089K

[13] N. C. Reichardt, M. Martin-Lomas, and S. Penades, Glyconanotechnology, Chem. Soc. Rev., 42 (2013) 4358-4376. https://doi.org/10.1039/C2CS35427F

[14] S. Cecioni, A. Imberty and S. Vidal, Glycomimetics Versus Multivalent Glycoconjugates for the Design of High Affinity Lectin Ligands, Chem. Rev., 115 (2015) 525-561. DOI: 10.1021/cr500303t

[15] M. Sánchez-Navarro, J. Rojo, Targeting DC-SIGN with carbohydrate multivalent systems, Drug News Perspect 23(9) (2010) 557-572. DOI: 10.1358/dnp.2010.23.9.1437246

[16] A. Muñoz, D. Sigwalt, B.M. Illescas, J. Luczkowiak, L. Rodríguez-Pérez, I. Nierengarten, M. Holler, J.-S. Remy, K. Buffet, S.P. Vincent, J. Rojo, R. Delgado, J.-F. Nierengarten, N. Martín, Synthesis of giant globular multivalent glycofullerenes as potent inhibitors in a model of Ebola virus infection, Nat Chem 8(1) (2016) 50-57. https://doi.org/10.1038/nchem.2387

[17] J. Ramos-Soriano, J.J. Reina, B.M. Illescas, N. de la Cruz, L. Rodríguez-Pérez, F. Lasala, J. Rojo, R. Delgado, N. Martín, Synthesis of Highly Efficient Multivalent Disaccharide/[60]Fullerene Nanoballs for Emergent Viruses, J. Am. Chem. Soc. 141(38) (2019) 15403-15412. https://doi.org/10.1021/jacs.9b08003

[18] B. M. Illescas, J. Rojo, R. Delgado and N. Martín, Multivalent Glycosylated Nanostructures To Inhibit Ebola Virus Infection, J. Am. Chem. Soc., 139, (2017) 6018-6025. https://doi.org/10.1021/jacs.7b01683

[19] L. Rodríguez-Pérez, J. Ramos-Soriano, A. Pérez-Sánchez, B.M. Illescas, A. Muñoz, J. Luczkowiak, F. Lasala, J. Rojo, R. Delgado, N. Martín, Nanocarbon-Based Glycoconjugates as Multivalent Inhibitors of Ebola Virus Infection, J. Am. Chem. Soc. 140(31) (2018) 9891-9898. https://pubs.acs.org/doi/10.1021/jacs.8b03847

[20] P. Guo, D. Liu, K. Subramanyam, B. Wang, J. Yang, J. Huang, D.T. Auguste, M.A. Moses, Nanoparticle elasticity directs tumor uptake, Nat. Commun. 9(1) (2018) 130. https://doi.org/10.1038/s41467-017-02588-9

[21] Camaleño de la Calle, A., Gerke, C., Chang, X. J., Grafmüller, A., Hartmann, L., Schmidt, S., Multivalent Interactions of Polyamide Based Sequence-Controlled Glycomacromolecules with Concanavalin A. Macromol. Biosci. 2019, 19, 1900033. https://doi.org/10.1002/mabi.201900033

[22] Shamout, F., Monaco, A., Yilmaz, G., Becer, C. R., Hartmann, L., Synthesis of Brush-Like Glycopolymers with Monodisperse, Sequence-Defined Side Chains and Their Interactions with Plant and Animal Lectins. Macromol. Rapid Commun. 2020, 41, 1900459. https://doi.org/10.1002/marc.201900459

[23] A.M. Caminade, S. Fruchon, C.O. Turrin, M. Poupot, A. Ouali, A. Maraval, M. Garzoni, M. Maly, V. Furer, V. Kovalenko, J.P. Majoral, G.M. Pavan, R. Poupot, The key role of the scaffold on the efficiency of dendrimer nanodrugs, Nat. Commun. 6 (2015) 7722. https://doi.org/10.1038/ncomms8722

[24] R.T. Chacko, J. Ventura, J. Zhuang, S. Thayumanavan, Polymer nanogels: A versatile nanoscopic drug delivery platform, Adv. Drug Deliv. Rev. 64(9) (2012) 836-851. https://doi.org/10.1016/j.addr.2012.02.002

[25] M. Asadian-Birjand, A. Sousa-Herves, D. Steinhilber, J.C. Cuggino, M. Calderon, Functional Nanogels in Biomedical Applications, Curr Med Chem 19 (2012) 5029-5043. https://doi.org/10.2174/092986731120902502 9

[26] A.V. Kabanov, S.V. Vinogradov, Nanogels as Pharmaceutical Carriers: Finite Networks of Infinite Capabilities, Angew. Chem. Int. Ed. 48(30) (2009) 5418-5429. https://doi.org/10.1002/anie.200900441

[27] M. Ahmed, P. Wattanaarsakit, R. Narain, Cationic glyco-nanogels for epidermal growth factor receptor (EGFR) specific siRNA delivery in ovarian cancer cells, Polym. Chem. 4(13) (2013) 3829-3836. https://doi.org/10.1039/C3PY00425B

[28] M.H. Smith, L.A. Lyon, Multifunctional Nanogels for siRNA Delivery, Acc. Chem. Res. 45(7) (2012) 985-993. https://doi.org/10.1021/ar200216f
[29] A. E. Ekkelenkamp, M. R. Elzes, J. F. J. Engbersen, and J. M. J. Paulusse, Responsive crosslinked polymer nanogels for imaging and therapeutics delivery, J. Mat. Chem. B, 6 (2018) 210-235. https://doi.org/10.1039/C7TB02239E
[30] Y. Chen, D. Diaz-Dussan, Y.-Y. Peng, and R. Narain, Hydroxyl-Rich PGMA-Based Cationic Glycopolymers for Intracellular siRNA Delivery: Biocompatibility and Effect of Sugar Decoration Degree, Biomacromolecules, 20 (2019) 2068-2074. https://doi.org/10.1021/acs.biomac.9b00274
[31] R. De Coen, N. Vanparijs, M.D.P. Risseeuw, L. Lybaert, B. Louage, S. De Koker, V. Kumar, J. Grooten, L. Taylor, N. Ayres, S. Van Calenbergh, L. Nuhn, B.G. De Geest, pH-Degradable Mannosylated Nanogels for Dendritic Cell Targeting, Biomacromolecules, 17 (2016) 2479-2488. https://doi.org/10.1021/acs.biomac.6b00685
[32] I. Papp, C. Sieben, A.L. Sisson, J. Kostka, C. Böttcher, K. Ludwig, A. Herrmann, R. Haag, Inhibition of Influenza Virus Activity by Multivalent Glycoarchitectures with Matched Sizes, ChemBioChem, 12 (2011) 887-895. https://doi.org/10.1002/cbic.201000776
[33] A.L. Martin, B. Li, E.R. Gillies, Surface functionalization of nanomaterials with dendritic groups: toward enhanced binding to biological targets, J. Am. Chem. Soc. 131 (2009) 734-741. https://doi.org/10.1021/ja807220u
[34] A. Sousa-Herves, R. Riguera, E. Fernandez-Megia, PEG-dendritic block copolymers for biomedical applications, New J. Chem. 36 (2012) 205–210. https://doi.org/10.1039/C2NJ20849K
[35] F. Wurm, H. Frey, Linear-dendritic block copolymers: The state of the art and exciting perspectives, Prog. Polym. Sci. 36 (2011) 1-52. https://doi.org/10.1016/j.progpolymsci.2010.07.009
[36]Knop K, Hoogenboom R, Fischer D, Schubert US. Poly(ethylene glycol) in drug delivery: pros and cons as well as potential alternatives. Angew Chem Int Ed Engl. 2010;49(36):6288-6308. doi:10.1002/anie.200902672
[37] G. Pasut, F.M. Veronese, PEG conjugates in clinical development or use as anticancer agents: An overview, Adv. Drug Deliv. Rev. 61 (2009) 1177-1188.
[38] E. Lallana, F. Fernandez-Trillo, A. Sousa-Herves, R. Riguera, E. Fernandez-Megia, Click Chemistry with Polymers, Dendrimers, and Hydrogels for Drug Delivery, Pharm. Res. 29(2012) 902-921. https://doi.org/10.1007/s11095-012-0683-y
[39] V.V. Rostovtsev, L.G. Green, V.V. Fokin, K.B. Sharpless, A Stepwise Huisgen Cycloaddition Process: Copper(I)-Catalyzed Regioselective "Ligation" of Azides and Terminal Alkynes, Angew. Chem. Int. Ed. 41 (2002) 2596-2599. https://doi.org/10.1002/1521-3773(20020715)41:14<2596::AID-ANIE2596>3.0.CO;2-4
[40] R. Ribeiro-Viana, J.J. García-Vallejo, D. Collado, E. Pérez-Inestrosa, K. Bloem, Y. van Kooyk, J. Rojo, BODIPY-Labeled DC-SIGN-Targeting Glycodendrons Efficiently Internalize and Route to Lysosomes in Human Dendritic Cells, Biomacromolecules 13 (2012) 3209-3219. https://doi.org/10.1021/bm300998c
[41] K. Landfester, Miniemulsion Polymerization and the Structure of Polymer and Hybrid Nanoparticles, Angew. Chem. Int. Ed. 48 (2009) 4488-4507. https://doi.org/10.1002/anie.200900723
[42] D. Steinhilber, S. Seiffert, J. A. Heyman, F. Paulus, D. A. Weitz, and R. Haag, Hyperbranched polyglycerols on the nanometer and micrometer scale, Biomaterials, 32 (2011) 1311-1316. https://doi.org/10.1016/j.biomaterials.2010.10.010
[43] A.A. Albalasmeh, A.A. Berhe, T.A. Ghezzehei, A new method for rapid determination of carbohydrate and total carbon concentrations using UV spectrophotometry, Carbohydrate Polymers 97(2) (2013) 253-261. https://doi.org/10.1016/j.carbpol.2013.04.072
[44] K.H. Schlick, J.R. Morgan, J.J. Weiel, M.S. Kelsey, M.J. Cloninger, Clusters of ligands on dendrimer surfaces, Bioorg. Med. Chem. Lett. 21(17) (2011) 5078-5083. https://doi.org/10.1016/j.bmcl.2011.03.100
[45] R. Ribeiro-Viana, M. Sánchez-Navarro, J. Luczkowiak, J.R. Koeppe, R. Delgado, J. Rojo, B.G. Davis, Virus-like glycodendrinanoparticles displaying quasi-equivalent nested polyvalency upon glycoprotein platforms potently block viral infection, Nat. Commun. 3 (2012) 1303. https://doi.org/10.1038/ncomms2302
[46] E. Arce, P.M. Nieto, V. Díaz, R.G. Castro, A. Bernad, J. Rojo, Glycodendritic Structures Based on Boltorn Hyperbranched Polymers and Their Interactions with Lens culinaris Lectin, Bioconj. Chem. 14(4) (2003) 817-823. https://doi.org/10.1021/bc034008k